

# Independent Component Analysis and (Simultaneous) Third-Order Tensor Diagonalization

Lieven De Lathauwer, Bart De Moor, *Senior Member, IEEE*, and Joos Vandewalle, *Fellow, IEEE*

**Abstract**—Comon’s well-known scheme for independent component analysis (ICA) is based on the maximal diagonalization, in a least-squares sense, of a higher-order cumulant tensor. In a previous paper, we proved that for fourth-order cumulants, the computation of an elementary Jacobi rotation is equivalent to the computation of the best rank-1 approximation of a fourth-order tensor. In this paper, we show that for third-order tensors, the computation of an elementary Jacobi-rotation is again equivalent to a best rank-1 approximation; however, here, it is a matrix that has to be approximated. This favorable computational load makes it attractive to do “something third-order-like” for fourth-order cumulant tensors as well. We show that simultaneous optimal diagonalization of “third-order tensor slices” of the fourth-order cumulant is a suitable strategy. This “simultaneous third-order tensor diagonalization” approach (STOTD) is similar in spirit to the efficient JADE-algorithm.

**Index Terms**—Eigenvalue decomposition, higher order statistics, independent component analysis, multilinear algebra, principal component analysis.

## I. INTRODUCTION

LET us use the following notation for the basic *independent component analysis* (ICA) or *blind source separation* (BSS) model:

$$Y = \mathbf{M}X + N = \tilde{Y} + N \quad (1)$$

in which the observation vector  $Y \in \mathbb{R}^I(\mathbb{C}^I)$ , the noise vector  $N \in \mathbb{R}^I(\mathbb{C}^I)$ , and the source vector  $X \in \mathbb{R}^J(\mathbb{C}^J)$  are zero-mean stochastic vectors, with  $I \geq J$ ; the mixing matrix  $\mathbf{M} \in \mathbb{R}^{I \times J}(\mathbb{C}^{I \times J})$  is assumed to be regular;  $\tilde{Y}$  is the signal part of the observations. The goal is to exploit the assumed mutual sta-

tistical independence of the source components to estimate the mixing matrix and/or the source signals from realizations of  $Y$ .

Our algorithm belongs to the class of prewhitening-based ICA algorithms. An eigenvalue decomposition (EVD) of the observed covariance matrix, or a singular value decomposition (SVD) of the data matrix, allows estimation of the number of sources and decorrelation of them; the remaining rotational degree of freedom is fixed by resorting to the higher order statistics (HOS) of the observations. Formally, if  $\hat{\mathbf{M}} = \mathbf{E} \cdot \mathbf{D} \cdot \mathbf{Q}$ , with  $\mathbf{E}$  and  $\mathbf{Q}$  orthogonal (unitary) and  $\mathbf{D}$  diagonal, is a singular value decomposition (SVD) of the mixing matrix estimate, then  $\mathbf{E}$  and  $\mathbf{D}$  are estimated in the prewhitening stage, and  $\mathbf{Q}$  is estimated in a higher order stage.  $\mathbf{Q}$  is estimated on the basis of the hypothesized standardized data model

$$Z = \mathbf{Q}X + N' \quad (2)$$

in which  $Z = \mathbf{D}^\dagger \mathbf{E}^H Y$  and  $N' = \mathbf{D}^\dagger \mathbf{E}^H N$ , with  $\dagger$  indicating the Moore–Penrose pseudo inverse and  $\cdot^H$  the (complex conjugated) transpose.

Up to some perturbation caused by non-Gaussian noise components, which are assumed to be small, the higher order cumulant of the standardized random vector  $Z$ ,  $\mathcal{C}_K^Z$  is a multilinear transformation of the higher order cumulant of the sources  $\mathcal{C}_K^X$ , e.g., for the fourth-order cumulants of complex-valued signals, assuming the complex conjugation pattern  $\mathcal{C}_4^Z = \text{Cum}\{Z, Z^*, Z^*, Z\}$ , i.e.,

$$(\mathcal{C}_4^Z)_{j_1 j_2 j_3 j_4} = \text{Cum}\{z_{j_1}, z_{j_2}^*, z_{j_3}^*, z_{j_4}\} \quad (3)$$

for all index entries, we have approximately

$$(\mathcal{C}_4^Z)_{j_1 j_2 j_3 j_4} = \sum_{k_1, k_2, k_3, k_4} (\mathcal{C}_4^X)_{k_1 k_2 k_3 k_4} q_{j_1 k_1} q_{j_2 k_2}^* q_{j_3 k_3}^* q_{j_4 k_4} \quad (4)$$

(From now on, we will denote such a multiplication by the short-hand notation  $\mathcal{C}_4^Z = \mathcal{C}_4^X \times_1 \mathbf{Q} \times_2 \mathbf{Q}^* \times_3 \mathbf{Q}^* \times_4 \mathbf{Q}$ .) The source cumulant is theoretically a diagonal tensor, i.e., the only nonvanishing entries have identical indices. To mitigate the fact that our assumptions are only approximately satisfied for the sample cumulants, [6] proposed to diagonalize the estimated cumulant of  $Z$  as far as possible, in a least-squares sense, i.e.,  $\mathbf{Q}$  is estimated as the orthogonal (unitary) matrix for which

$$f(\hat{X}) = \sum_{j=1}^J \left| (\mathcal{C}_K^{\hat{X}})_{jj\dots j} \right|^2 \quad (5)$$

is maximized, where  $\hat{X}$  is the corresponding source estimate.  $\mathbf{Q}$  is obtained by Jacobi iteration. It is estimated as a product

Manuscript received July 28, 2000; revised July 2, 2001. This work was supported by the Research Council KU Leuven: Concerted Research Action GOA-MEFISTO-666 (Mathematical Engineering for Information and Communication Systems Technology), the FWO Projects G.0240.99 (Multilinear Generalizations of the Singular Value Decomposition and Applications in Signal Processing and System Identification) and G.0256.97 (Numerical Algorithms for Subspace System Identification, Extension to Special Cases), the FWO Research Communities Identification and Control of Complex Systems (ICCoS) and Advanced Numerical Methods for Mathematical Modeling (ANMMM), project BIL 98 with South Africa, and the Belgian State, Prime Minister’s Office—Federal Office for Scientific, Technical, and Cultural Affairs—Interuniversity Poles of Attraction Programme [IUAP P4-02 (1997-2001): Modeling, Identification, Simulation, and Control of Complex Systems and IUAP P4-24 (1997-2001): Intelligent Mechatronic Systems (IMechS)]. The associate editor coordinating the review of this paper and approving it for publication was Prof. Hideaki Sakai.

L. De Lathauwer is with the ETIS, UPRES-A 8051, Cergy-Pontoise, France, and with SISTA/COSIC, ESAT, Katholieke Universiteit Leuven, Leuven, Belgium (e-mail: delathau@esat.kuleuven.ac.be; lathauwr@ensea.fr).

B. De Moor and J. Vandewalle are with SISTA/COSIC, ESAT, Katholieke Universiteit Leuven, Leuven, Belgium (e-mail: demoor@esat.kuleuven.ac.be; vdwalle@esat.kuleuven.ac.be).

Publisher Item Identifier S 1053-587X(01)08244-7.

of elementary Jacobi rotations, where each elementary rotation diagonalizes, as far as possible, the  $(2 \times 2 \times \dots \times 2)$  subtensor associated with the marginal cumulants of the estimates of two different source components.

In Section II, we reconsider the case of third-order cumulants and show that it leads to similar expressions as the ones obtained in the derivation of the JADE-algorithm [1]. In Section III, we generalize the results to ICA based on fourth-order cumulants or on a combination of third- and fourth-order cumulants. After deriving the concept, we investigate some properties of the new technique and illustrate its performance by means of a number of numerical experiments.

In [14], Moreau presents the idea of combining different cumulant orders in a JADE- or STOTD-type scheme. It is based on a preliminary version [8] of this paper; however, the current paper is the first elaborated version. Moreau [14] and Stoll and Moreau [15] are restricted to real-valued data, whereas in this paper, we also consider the case of complex-valued data.

## II. MAXIMAL DIAGONALIZATION OF A THIRD-ORDER TENSOR

In this section, we show that the computation of the Jacobi-rotation that maximally diagonalizes a given  $(2 \times 2 \times 2)$  cumulant tensor or a  $(2 \times 2 \times 2)$  tensor with the same symmetries (as in Section III) is equivalent to the best rank-1 approximation of a symmetric matrix. Both the real and complex case are studied.

Let us first consider the *real-valued case*. The  $(2 \times 2 \times 2)$  tensor to be diagonalized is called  $\tilde{\mathcal{C}}$ . It has the symmetries of a cumulant of which the entries are given by  $\text{Cum}\{\tilde{z}_i, \tilde{z}_j, \tilde{z}_k\}$ , i.e., it is invariant under arbitrary permutations of its indices; this property is called real super-symmetry. We define  $\mathcal{C} = \tilde{\mathcal{C}} \times_1 \mathbf{J} \times_2 \mathbf{J} \times_3 \mathbf{J}$  in which  $\mathbf{J}$  is a Givens rotation matrix, implementing an orthogonal basis transformation. We use the standard representation of Givens rotations

$$\mathbf{J} = \begin{pmatrix} \cos \alpha & -\sin \alpha \\ \sin \alpha & \cos \alpha \end{pmatrix}. \quad (6)$$

We construct a real symmetric  $(2 \times 2)$ -matrix  $\mathbf{B}$  as follows:

$$b_{11} = a_1 \quad (7)$$

$$b_{12} = 3a_4/2 \quad (8)$$

$$b_{22} = 9a_2/4 + 3a_3/2 + a_1/4 \quad (9)$$

in which the auxiliary variables  $a_1, a_2, a_3, a_4$  are given by

$$a_1 = \tilde{c}_{111}^2 + \tilde{c}_{222}^2 \quad (10)$$

$$a_2 = \tilde{c}_{112}^2 + \tilde{c}_{122}^2 \quad (11)$$

$$a_3 = \tilde{c}_{111}\tilde{c}_{122} + \tilde{c}_{112}\tilde{c}_{222} \quad (12)$$

$$a_4 = \tilde{c}_{122}\tilde{c}_{222} - \tilde{c}_{111}\tilde{c}_{112}. \quad (13)$$

Using these notations, we state the following.

*Theorem 1:* Assume a super-symmetric tensor  $\tilde{\mathcal{C}} \in \mathbb{R}^{2 \times 2 \times 2}$ , and consider the tensor  $\mathcal{C}$  and the matrix  $\mathbf{B}$ , which are defined above. The squared norm of the diagonal of  $\mathcal{C}$  is given by

$$\sum_{i=1}^2 c_{iii}^2 = U^T \cdot \mathbf{B} \cdot U \quad (14)$$

in which  $U \stackrel{\text{def}}{=} (\cos(2\alpha) \sin(2\alpha))^T$ .

*Proof:* The theorem can be proved with straightforward calculus. The main subresults are given in Appendix A. ■

Hence, the optimal rotation can be found by computing the dominant eigenvector of  $\mathbf{B}$  (i.e., the eigenvector corresponding to the eigenvalue having the largest absolute value) and normalizing it to unit length. The actual elements of the optimal inner Givens rotation can be obtained from the entries of  $U$  by using the basic goniometric relations  $\cos \alpha = (1 + \cos(2\alpha)/2)^{1/2}$  and  $\sin \alpha = \sin(2\alpha)/(2\cos \alpha)$ . It is clear that the function  $\sum_{i=1}^2 c_{iii}^2$  is periodic in the rotation angle, with period  $\pi/2$ , as the sign of  $U$  is of no importance. The sign of the dominant eigenvector can be fixed to restrict  $\mathbf{J}$  to the set of inner rotations ( $\alpha \in (-\pi/4, +\pi/4)$ ).

Starting from a different kind of parametrization of the Givens rotation matrix, Comon also found that in the real third-order case, the computation of the optimal rotation is a quadratic problem [5]. (For the real fourth-order case, the computation amounts to the rooting of a polynomial of degree 4.) However, this format shows less explicitly the analogy with the JADE-algorithm; see also Section III. The nontrivial derivation of the complex case, to be discussed below, is entirely new.

We also remark that generic real super-symmetric third-order tensors, as opposed to matrices, cannot be completely diagonalized. This can easily be verified by counting degrees of freedom; any diagonalizable real super-symmetric  $(2 \times 2 \times 2)$  tensor  $\tilde{\mathcal{C}}$  can by definition be written as  $\tilde{\mathcal{C}} = \mathcal{C} \times_1 \mathbf{J}^T \times_2 \mathbf{J}^T \times_3 \mathbf{J}^T$ , in which  $\mathcal{C}$  is diagonal and  $\mathbf{J}$  a Givens rotation; hence, the manifold of diagonalizable tensors is three dimensional (3-D), whereas the full vector space of real super-symmetric  $(2 \times 2 \times 2)$  tensors is four dimensional (4-D).

Now, let us consider the *complex-valued case*. We assume that the complex  $(2 \times 2 \times 2)$  tensor  $\tilde{\mathcal{C}}$  does not change when its second and third index are interchanged (like it is the case for a cumulant defined by the element-wise equation  $\tilde{c}_{ijk} = \text{Cum}(\tilde{z}_i, \tilde{z}_j^*, \tilde{z}_k^*)$  for some random vector  $\tilde{\mathbf{z}}$ ).

We define  $\mathcal{C} = \tilde{\mathcal{C}} \times_1 \mathbf{J} \times_2 \mathbf{J}^* \times_3 \mathbf{J}^*$  in which  $\mathbf{J}$  is a complex Givens rotation matrix. For  $\mathbf{J}$ , we use the standard representation

$$\mathbf{J} = \begin{pmatrix} \cos \alpha & -\sin \alpha e^{i\phi} \\ \sin \alpha e^{-i\phi} & \cos \alpha \end{pmatrix}. \quad (15)$$

We construct a real symmetric  $(3 \times 3)$  matrix  $\mathbf{B}$  as follows:

$$b_{11} = a_1 \quad (16)$$

$$b_{12} = \text{Im}(v_1) + \text{Im}(v_2) \quad (17)$$

$$b_{13} = \text{Re}(v_1) - \text{Re}(v_2) \quad (18)$$

$$b_{22} = v_4 - \text{Re}(v_3) \quad (19)$$

$$b_{23} = \text{Im}(v_3) \quad (20)$$

$$b_{33} = v_4 + \text{Re}(v_3) \quad (21)$$

in which  $\text{Re}(\cdot)$  and  $\text{Im}(\cdot)$  denote, respectively, the real and complex part of a complex number, and where the auxiliary variables are given by

$$a_1 = |\tilde{c}_{111}|^2 + |\tilde{c}_{222}|^2 \quad (22)$$

$$a_2 = |\tilde{c}_{112}|^2 + |\tilde{c}_{212}|^2 \quad (23)$$

$$a_3 = |\tilde{c}_{211}|^2 + |\tilde{c}_{122}|^2 \quad (24)$$

$$a_4 = \tilde{c}_{111}\tilde{c}_{112}^* \quad (25)$$

$$a_5 = \tilde{c}_{111}\tilde{c}_{211}^* \quad (26)$$

$$a_6 = \tilde{c}_{222}\tilde{c}_{122}^* \quad (27)$$

$$a_7 = \tilde{c}_{222}\tilde{c}_{212}^* \quad (28)$$

$$a_8 = \tilde{c}_{111}\tilde{c}_{212}^* + \tilde{c}_{222}\tilde{c}_{112}^* \quad (29)$$

$$a_9 = \tilde{c}_{111}\tilde{c}_{122}^* + \tilde{c}_{222}\tilde{c}_{211}^* \quad (30)$$

$$a_{10} = \tilde{c}_{211}^*\tilde{c}_{112} + \tilde{c}_{122}\tilde{c}_{212}^* \quad (31)$$

$$v_1 = a_7 - a_5/2 \quad (32)$$

$$v_2 = a_4 - a_6/2 \quad (33)$$

$$v_3 = a_9/2 + a_{10} \quad (34)$$

$$v_4 = (a_1 + a_3)/4 + a_2 + \text{Re}(a_8). \quad (35)$$

Using these notations, we state the following.

**Theorem 2:** Consider the complex-valued  $(2 \times 2 \times 2)$  tensor  $\tilde{\mathcal{C}}$ , the tensor  $\mathcal{C}$ , and the matrix  $\mathbf{B}$ , defined above. The squared norm of the diagonal of  $\mathcal{C}$  is given by

$$\sum_{i=1}^2 |c_{iii}|^2 = U^T \cdot \mathbf{B} \cdot U \quad (36)$$

in which  $U \stackrel{\text{def}}{=} (\cos(2\alpha) \sin(2\alpha) \sin \phi \sin(2\alpha) \cos \phi)^T$ .

*Proof:* The theorem can be proved with straightforward calculus. The main subresults are given in Appendix A. ■

It can easily be verified that the formulas for the complex case reduce to those for the real case if we assume that  $\phi = 0$  and that  $\tilde{\mathcal{C}}$  is real super-symmetric.

Like in the real case, the optimal rotation can be found by computing the dominant eigenvector of  $\mathbf{B}$  and normalizing it to unit length. The actual elements of the optimal inner Givens rotation can be obtained from the entries of  $U$  by using the basic relations  $\cos \alpha = \sqrt{1 + \cos(2\alpha)}/2$  and  $\sin \alpha e^{i\phi} = (\sin(2\alpha) \cos \phi + i \sin(2\alpha) \sin \phi)/(2 \cos \alpha)$ . The sign of the dominant eigenvector can be fixed to restrict  $\mathbf{J}$  to the set of inner rotations ( $\alpha \in (-\pi/4, +\pi/4]$ ).

$(K \times K \times K)$  tensors, with  $K > 2$ , can be maximally diagonalized by means of a Jacobi-type iteration. In our simulations, we have always observed convergence to the global optimum when the tensor can be exactly diagonalized. However, like for the Jacobi-techniques of e.g., [1], [6], a formal proof of convergence is lacking. When only approximate diagonalization is possible, we usually observe global convergence, but there are cases in which the global optimum is not found. This will be illustrated in Section III-D, as well as for the technique of [1].

The results of this section can be readily applied to estimate the factor  $\mathbf{Q}$  in the ICA problem, which was sketched in the introduction, provided at most one of the third-order cumulants of the sources is zero.

### III. ICA BY SIMULTANEOUS THIRD-ORDER TENSOR DIAGONALIZATION

In this section, we show that the results of the previous section, involving third-order tensors, can still be useful for ICA in which the higher order stage is based on fourth-order cumulants. This leads to a new technique, which will be referred to as ‘‘ICA by simultaneous third-order tensor diagonalization’’ (STOTD). In the first subsection, we explain the basics of this method. Sec-

tion III-B contains the algorithmic details. In Section III-C, we discuss some properties of the technique. Finally, Section III-D illustrates the performance with some simulations. An outline of the algorithm is presented as Algorithm 1.

Algorithm 1

*ICA by means of STOTD*

Given:  $N$  samples  $\{Y_n\}_{1 \leq n \leq N}$  of  $Y = \mathbf{M}X + N$ , as in (1). Let  $\tilde{\mathbf{M}} = \mathbf{E} \cdot \mathbf{D} \cdot \mathbf{Q}$  be an SVD of the mixing matrix estimate.

1. Determine  $\mathbf{E}, \mathbf{D}$  from a prewhitening.
2. Call  $\tilde{\mathcal{C}}_4^Z$  the sample cumulant of the whitened observations. Associate with  $\tilde{\mathcal{C}}_4^Z$  a linear mapping from  $\mathbb{R}^J(\mathbb{C}^J)$  to  $\mathbb{R}^{J \times J \times J}$  ( $\mathbb{C}^{J \times J \times J}$ ) [see (37)]. Determine a basis  $\{\mathcal{T}^{(l)}\}_{(1 \leq l \leq J)}$  of the range  $\mathbb{R}\{\tilde{\mathcal{C}}_4^Z\}$  (Section III-A).
3. Initialize  $\mathbf{Q} \leftarrow \mathbf{I}$  and  $\tilde{\mathcal{T}}^{(l)} \leftarrow \mathcal{T}^{(l)}$  ( $1 \leq l \leq J$ ). Sweep the  $J(J-1)$  pairs  $(i, j)$ , according to a fixed ordering. Iterate until convergence ( $|\alpha| < \epsilon$  for all rotation pairs). For each pair:
  - a) Call  $\tilde{\mathcal{C}}^{(l)}$  the  $(2 \times 2 \times 2)$ -subtensor of  $\tilde{\mathcal{T}}^{(l)}$  ( $1 \leq l \leq J$ ), corresponding to sources  $i$  and  $j$ . Construct symmetric matrix  $\mathbf{B} \in \mathbb{R}^{2 \times 2}$  in accordance with (7)–(9) and (43)–(46) (real case), or symmetric matrix  $\mathbf{B} \in \mathbb{R}^{3 \times 3}$  in accordance with (16)–(21) and (47)–(56) (complex case).
  - b) Determine  $U \in \mathbb{R}^2(\mathbb{R}^3)$ , with  $\|U\| = 1$  and  $u_1 \in \mathbb{R}^+$ , as the dominant eigenvector of  $\mathbf{B}$ .
  - c) Construct  $\mathbf{J}_{ij}$  from  $U$ , in accordance with Theorem 1 and (6) (real case), or in accordance with Theorem 2 and (15) (complex case).
  - d) Update  $\tilde{\mathcal{T}}^{(l)} \leftarrow \tilde{\mathcal{T}}^{(l)} \times_1 \mathbf{J}_{ij} \times_2 \mathbf{J}_{ij}^* \times_3 \mathbf{J}_{ij}^*$  ( $1 \leq l \leq J$ ).
  - e) Accumulate  $\mathbf{Q} \leftarrow \mathbf{Q} \cdot \mathbf{J}_{ij}^H$ .

#### A. Basic Idea

Consider the fourth-order cumulant tensor  $\mathcal{C}_4^Z$  of the standardized random vector  $Z$  in the higher order ICA stage, as in (4). Let us associate with  $\mathcal{C}_4^Z$  a linear transformation of  $\mathbb{C}^J$  to the vector space of third-order tensors  $\mathbb{C}^{J \times J \times J}$  in the following way

$$\mathcal{V} = \mathcal{C}_4^Z(V) \iff v'_{ijk} = \sum_l (\mathcal{C}_4^Z)_{ijkl} v_l \quad (37)$$

for all index values. This linear mapping has a very special structure if we neglect the additive noise term in the ICA-model. In terms of (4), the SVD of the mapping is given by

$$(\mathcal{C}_4^Z)_{pqrs} = \sum_j \sigma_j(Q_j)_{pqr}(Q_j)_s \quad (38)$$

in which we have the following.

- The singular values are given by  $\text{sign}(\kappa_j^X)\kappa_j^X$  ( $1 \leq j \leq J$ ), where  $\kappa_j^X$  symbolizes the kurtosis of the  $j$ th source.
- The corresponding right singular vectors  $Q_j^*$  are the columns of  $\mathbf{Q}$ , represented by  $Q_j$  ( $1 \leq j \leq J$ ), and complex conjugated by convention.

- The corresponding “left singular tensors”  $\mathcal{Q}_j$  ( $1 \leq j \leq J$ ) are given by

$$(\mathcal{Q}_j)_{pqr} = \text{sign}(\kappa_j^X) (\mathcal{Q}_j)_p (\mathcal{Q}_j)_q^* (\mathcal{Q}_j)_r^*. \quad (39)$$

Therefore, the SVD of the linear mapping is strongly related to the standardized mixing matrix  $\mathbf{Q}$ . Moreover, we remark that all the third-order tensors in the range space of  $\mathcal{C}_4^Z$  can be written as a linear combination of the left singular tensors such that they can be diagonalized by  $\mathbf{Q}$ .

When noise is present and/or when the statistics of  $Z$  are only available with limited accuracy, the derivation above is only approximately valid. We propose to estimate  $\mathbf{Q}$  as the unitary (orthogonal) matrix that simultaneously diagonalizes as far as possible (in least-squares sense) a set of third-order tensors that form a basis for the range of  $\mathcal{C}_4^Z$ . Formally, if the set to be diagonalized is given by  $\{\mathcal{T}^{(l)}\}_{(1 \leq l \leq J)}$ ,  $\mathbf{Q}$  is estimated as the unitary (orthogonal) matrix  $\mathbf{U}$  that maximizes the function

$$f(\mathbf{U}) = \sum_l \left( \sum_n |t'_{nnn}^{(l)}|^2 \right) \quad (40)$$

where  $\mathcal{T}'^{(l)}$  equals the tensor  $\mathcal{T}^{(l)}$  after multiplication with  $\mathbf{U}$ :

$$\mathcal{T}'^{(l)} = \mathcal{T}^{(l)} \times_1 \mathbf{U} \times_2 \mathbf{U}^* \times_3 \mathbf{U}^*. \quad (41)$$

By simultaneously diagonalizing a full basis of the range of  $\mathcal{C}_4^Z$ , the information contained in all the entries of  $\mathcal{C}_4^Z$  can be exploited. An orthogonal basis for the range of the linear mapping can be obtained from the SVD in (38), together with a first estimate of  $\mathbf{Q}$ . Therefore, for the set to be jointly diagonalized, one could take the set of left singular tensors  $\{\mathcal{Q}_j\}_{(1 \leq j \leq J)}$ . On the other hand, the first terms in (38) have a larger contribution to  $\mathcal{C}_4^Z$  than the last ones (we assume that the singular values are listed in decreasing order). To take into account the relative importance of the different terms, it makes sense to jointly diagonalize the set  $\{\kappa_i^X \mathcal{Q}_j\}_{(1 \leq j \leq J)}$  instead. This corresponds to the optimization of the weighted function

$$f(\mathbf{U}) = \sum_l (\kappa_l^X)^2 \left( \sum_n |(\mathcal{Q}_j)_{nnn}^{(l)}|^2 \right). \quad (42)$$

One could also “roughly” resort to an ordinary basis that is obtained by simple transformation under  $\mathcal{C}_4^Z$  of  $J$  linearly independent vectors, e.g., transformation of the canonical unit vectors corresponds to choosing the “third-order tensor slices”  $(\mathcal{C}_4^Z)^{(l)}$ , which are obtained by keeping the index  $l$  in  $(\mathcal{C}_4^Z)_{ijkl}$  fixed.

### B. Computation

Like for the optimal diagonalization of a single third-order tensor, the optimal simultaneous diagonalization of a set of third-order tensors will be computed by Jacobi-iteration. In each step the set of  $J$  ( $2 \times 2 \times 2$ )-tensors associated with the elementary rotation, will be diagonalized as far as possible. This set will be represented by  $\{\tilde{\mathcal{C}}^{(l)}\}_{(1 \leq l \leq J)}$ . By Jacobi-rotation these tensors are transformed into the set  $\{\mathcal{C}^{(l)}\}_{(1 \leq l \leq J)}$ .

The function that will be maximized is the sum of the squared norms of the diagonals of the tensors  $\mathcal{C}^{(l)}$ . Theorems 1 and 2 show that the optimal rotation can still be estimated via the dominant eigenvector of a real symmetric ( $2 \times 2$ )-matrix (real case)

or a real symmetric ( $3 \times 3$ )-matrix (complex case); however, the matrix itself is computed as a sum of contributions of the individual tensors.

As far as *real-valued tensors* are concerned, this boils down to replacing the definitions of  $a_1$  to  $a_4$  in (10)–(13) by the following summations:

$$a_1 = \sum_l \left( \tilde{c}_{111}^{(l)} \right)^2 + \left( \tilde{c}_{222}^{(l)} \right)^2 \quad (43)$$

$$a_2 = \sum_l \left( \tilde{c}_{112}^{(l)} \right)^2 + \left( \tilde{c}_{122}^{(l)} \right)^2 \quad (44)$$

$$a_3 = \sum_l \tilde{c}_{111}^{(l)} \tilde{c}_{122}^{(l)} + \tilde{c}_{112}^{(l)} \tilde{c}_{222}^{(l)} \quad (45)$$

$$a_4 = \sum_l \tilde{c}_{122}^{(l)} \tilde{c}_{222}^{(l)} - \tilde{c}_{111}^{(l)} \tilde{c}_{112}^{(l)}. \quad (46)$$

In the *complex case*, the definitions of  $a_1$  to  $a_{10}$  in (22)–(31) have to be modified to

$$a_1 = \sum_l \left| \tilde{c}_{111}^{(l)} \right|^2 + \left| \tilde{c}_{222}^{(l)} \right|^2 \quad (47)$$

$$a_2 = \sum_l \left| \tilde{c}_{112}^{(l)} \right|^2 + \left| \tilde{c}_{212}^{(l)} \right|^2 \quad (48)$$

$$a_3 = \sum_l \left| \tilde{c}_{211}^{(l)} \right|^2 + \left| \tilde{c}_{122}^{(l)} \right|^2 \quad (49)$$

$$a_4 = \sum_l \tilde{c}_{111}^{(l)} \left( \tilde{c}_{112}^{(l)} \right)^* \quad (50)$$

$$a_5 = \sum_l \tilde{c}_{111}^{(l)} \left( \tilde{c}_{211}^{(l)} \right)^* \quad (51)$$

$$a_6 = \sum_l \tilde{c}_{222}^{(l)} \left( \tilde{c}_{122}^{(l)} \right)^* \quad (52)$$

$$a_7 = \sum_l \tilde{c}_{222}^{(l)} \left( \tilde{c}_{212}^{(l)} \right)^* \quad (53)$$

$$a_8 = \sum_l \tilde{c}_{111}^{(l)} \left( \tilde{c}_{212}^{(l)} \right)^* + \tilde{c}_{222}^{(l)} \left( \tilde{c}_{112}^{(l)} \right)^* \quad (54)$$

$$a_9 = \sum_l \left( \tilde{c}_{111}^{(l)} \right)^* \tilde{c}_{122}^{(l)} + \tilde{c}_{222}^{(l)} \left( \tilde{c}_{211}^{(l)} \right)^* \quad (55)$$

$$a_{10} = \sum_l \left( \tilde{c}_{211}^{(l)} \right)^* \tilde{c}_{112}^{(l)} + \tilde{c}_{122}^{(l)} \left( \tilde{c}_{212}^{(l)} \right)^*. \quad (56)$$

*Remark 1:* Although this result might seem contrainuitive, it turns out now that simultaneous diagonalization of a set of third-order tensors, exhibiting the symmetries specified above, leads to a similar expression as the simultaneous diagonalization of a set of Hermitean (symmetric) matrices; cf. [1].

In the same way, one can base the higher order step of the algorithm on third- and fourth-order cumulants. Therefore, one can add (a weighted version) of the third-order cumulant to the set of third-order tensors that has to be diagonalized. One should then simply consider a matrix  $\mathbf{B}$  ((7)–(9) or (16)–(21)) that consists of a weighted sum of contributions related to the third- and fourth-order cumulant. In this way, it becomes possible to separate sources that are nonkurtic, provided their skewness is different from zero, and vice versa. This idea was proposed in [14], where it was called “extended STOTD” (eSTOTD); this paper was based on the preliminary paper [8].

### C. Properties

In this subsection, we will study two interesting properties of the STOTD technique. First, we will show that the technique can be cast in the framework of contrast optimization. Second, we will demonstrate that the STOTD estimator is invariant w.r.t. left multiplication of the mixing matrix by a square regular matrix.

1) *Contrast Optimization*: In several ICA techniques, the mixing matrix is estimated through the optimization of a so-called *contrast function* (cf. definition proposed in [4] and [6]; this definition was generalized in [13]).

*Definition 1 (Contrast)*: A contrast over a set  $\mathcal{M}$  of matrices is a mapping  $\Psi$  from the set of probability densities  $\{p_X | X \in \mathbb{C}^J \text{ or } \mathbb{R}^J\}$  to  $\mathbb{R}$  that satisfies the following requirements.

- 1)  $\Psi(p_X)$  does not change if the components of  $X$  are permuted or scaled

$$\Psi(p_X) = \Psi(p_{\mathbf{A}\mathbf{P}X}) \quad (57)$$

in which  $\mathbf{A}$  is a diagonal matrix and  $\mathbf{P}$  a permutation matrix.

- 2) If  $X$  has mutually independent components, then  $\Psi(p_{\mathbf{M}X}) \leq \Psi(p_X)$  for every matrix  $\mathbf{M} \in \mathcal{M}$ .
- 3) If  $X$  has mutually independent components, then  $\Psi(p_{\mathbf{M}X}) = \Psi(p_X)$  only if  $\mathbf{M} = \mathbf{A}\mathbf{P}$ , where  $\mathbf{A}$  is a diagonal matrix and  $\mathbf{P}$  a permutation matrix.

The first condition reflects that contrast optimization should show the same indeterminacies as ICA itself. The basis of contrast optimization is established by condition 2; uniqueness is obtained by the third condition. Property 3 is referred to as the *discrimination property* of the contrast function.

The notation  $\Psi(p_X)$  is often abbreviated as  $\Psi(X)$ .

We now show the following theorem.

*Theorem 3 (Contrast)*: Let  $\mathcal{C}_4^X$  be the fourth-order cumulant of a white stochastic vector  $X$  with values in  $\mathbb{C}^J$  ( $\mathbb{R}^J$ ). The function

$$f(X) = \sum_{l=1}^J \sum_{j=1}^J \left| (\mathcal{C}_4^X)_{jjjl} \right|^2 \quad (58)$$

is a contrast function over the manifold of unitary (orthogonal) matrices. It is discriminating for the set of random vectors of which at most one component has zero kurtosis.

*Proof*: The proof is given in Appendix A. ■

In [15], a class of contrasts is proposed that encompasses contrast (58). The paper by Stoll and Moreau [15] was based on the preliminary paper [8].

2) *Invariance*: Invariance of an ICA estimator means that in the absence of noise, its estimates are transformed in the same way as the mixing matrix when multiplied from the left with a regular matrix  $\mathbf{A}$ . The interference-to-signal ratio (ISR) obtained by invariant ICA estimators does not depend on the mixing matrix; it can even be computed using the unmixed dataset (still under the no-noise assumption). This property is called uniform performance of invariant estimators [2].

For details on the general theory of invariance, see [11, ch. 6]. For aspects of invariance related to ICA, see [3]. We now state that the STOTD-technique is an invariant ICA estimator.

*Theorem 4 (Invariant Estimator)*: The two-stage ICA-procedure, based on prewhitening and simultaneous diagonalization

of the third-order tensor slices of the standardized fourth-order cumulant tensor, is an invariant estimator of the mixing matrix.

*Proof*: The proof is given in Appendix A. ■

### D. Simulations

We illustrate the performance of the STOTD technique by means of three Monte Carlo experiments, in which we average over 500 simulations. In each of the figures, the solid lines are obtained by STOTD. The dashed lines, which are drawn for comparison, are obtained by means of the JADE algorithm [1].

In a first experiment, we consider a setup of two observation channels, listening to two sources, in which the signals are real valued. Three different types of zero-mean unit-variance source distributions are used:

- a) binary distribution, with  $\text{Prob}(x = 1) = \text{Prob}(x = -1) = 1/2$ ;
- b) uniform distribution over the interval  $[-\sqrt{3}, +\sqrt{3}]$ ;
- c) double-sided exponential distribution  $p_X(x) = (1/\sqrt{2}) \exp(-\sqrt{2}|x|)$ .

The three possible configurations (binary/uniform, binary/double-sided exponential, and uniform/double-sided exponential) are considered. Since the three distributions are even, the higher order stage of the algorithm is based on the fourth-order cumulant. In each simulation, a new mixing matrix is generated by taking its elements from a zero-mean Gaussian distribution. The columns of the mixing matrix are subsequently scaled to unit length. In this first experiment, the additive noise term  $N$  is neglected.

We consider the following two indices of performance. First,  $\text{ISR}_{ij} \stackrel{\text{def}}{=} \mathbb{E}\{|\hat{\mathbf{M}}^\dagger \mathbf{M}\}_{ij}|^2\}$  quantifies the average contamination by the  $j$ th source of the  $i$ th source estimate and can be considered to be an (approximate) ISR. Secondly, we consider the root mean square error (RMSE)  $\sqrt{\mathbb{E}\|\mathbf{M} - \hat{\mathbf{M}}\|^2}$  in which both matrices are normalized in the same way. For  $\mathbf{M}$ , we assume unit-variance sources, and for  $\hat{\mathbf{M}}$ , we assume the corresponding optimal column ordering and scaling. These performance parameters are plotted as a function of the length of the datasets  $T$ .

In Fig. 1, we plot the mean ISR for the three source configurations. The dotted line is the theoretical low-noise upper-bound of performance given by [2, eq. (30)]

$$\lim_{T \rightarrow \infty, \sigma_N \rightarrow 0} \text{TE}\{\text{ISR}_{21} + \text{ISR}_{12}\} \geq \frac{1}{2} \quad (59)$$

in which  $\sigma_N$  is the standard deviation of spatially and temporally white Gaussian noise.

In Fig. 2, we plot the RMSE. The dash-dotted and dotted lines give the two upper bounds of performance derived in [10]. The dash-dotted lines image the performance that could ultimately be obtained given the error introduced in the prewhitening step; the dotted lines show the ultimate performance when only taking into account the estimation error on the singular values of the mixing matrix.

The second experiment is inspired by the simulations described in [1]. We consider two zero-mean complex-valued source signals drawn from a uniform distribution over the circle with unit radius. Both signals impinge on a linear  $\lambda/2$  equispaced array of 10 unit-gain omnidirectional sensors in the far field of the emitters. The theoretical values of the elements

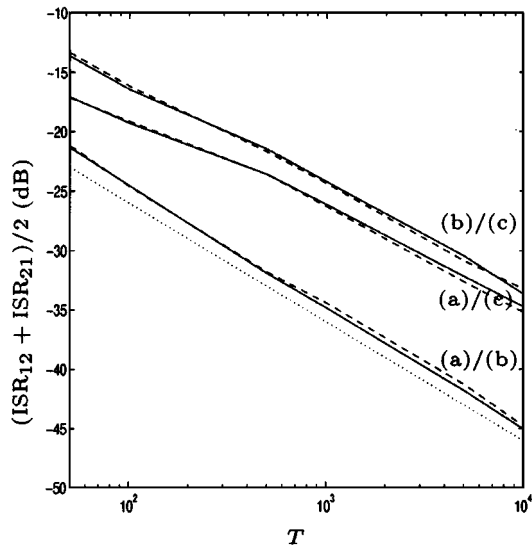


Fig. 1. Mean ISR in the first simulation of Section III-D, as a function of the length of the dataset  $T$ . Configurations of the source distributions. (a) Binary. (b) Uniform. (c) Double-sided exponential. Solid: The mixing matrix is estimated by means of the STOTD technique. Dashed: The mixing matrix is estimated by means of the JADE technique. Dotted: Upper bound of performance.

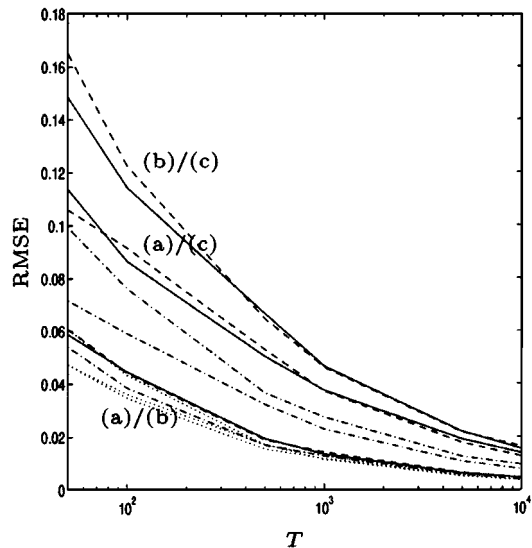


Fig. 2. RMSE in the first simulation of Section III-D, as a function of the length of the dataset  $T$ . Configurations of the source distributions. (a) Binary. (b) Uniform. (c) Double-sided exponential. Solid: The mixing matrix is estimated by means of the STOTD technique. Dashed: The mixing matrix is estimated by means of the JADE technique. Dash-dotted: The upper bound of performance given by [10, eq. (20)]. Dotted: The upper bound of performance given by [10, eq. (21)].

of the mixing matrix are given by  $m_{pq} = e^{2j\pi p\phi_q}$ , where  $\phi_q$  equals the electrical angle of source  $q$ . The noise is Gaussian, with power  $\sigma_N^2$ . In each experiment, the data length  $T = 100$ , and the angle  $\phi_1 = 0$ . Since the source distributions are point symmetric around the origin, the higher order stage of the algorithm is based on the fourth-order cumulant.

In Fig. 3, we plot the mean ISR. The top figure shows the effect of a varying signal-to-noise ratio (SNR) for three different mixing configurations  $\phi_2 = 0.02, 0.05$  and  $0.1$  (note that in the latter case, the steering vectors are mutually orthogonal). The bottom figure shows the effect of the difference in direction-of-

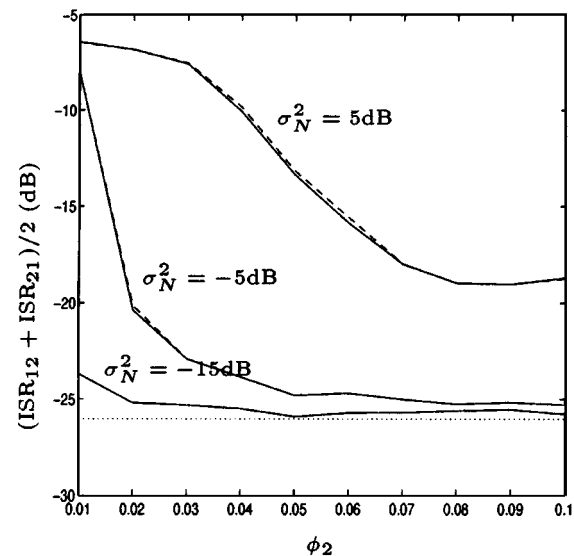
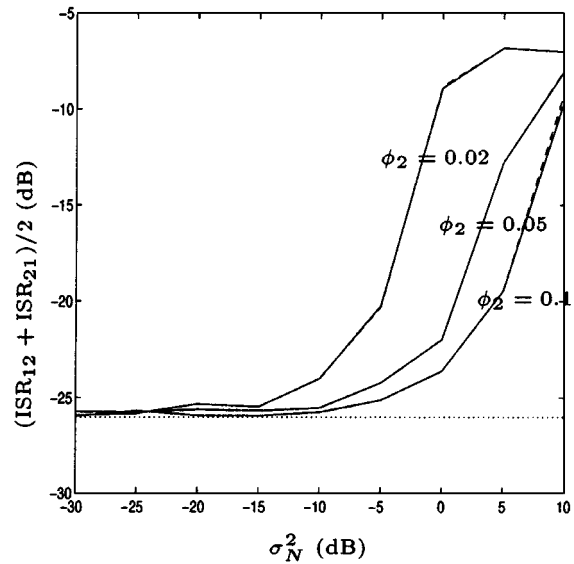


Fig. 3. Mean ISR in the second simulation of Section III-D. Solid: The mixing matrix is estimated by means of the STOTD technique. Dashed: The mixing matrix is estimated by means of the JADE technique. Dotted: Low-noise upper-bound of performance. *Top*: Effect of the SNR on the quality of separation.  $\phi_1 = 0$ . *Bottom*: Effect of the difference in DOA ( $\phi_1 = 0$ ) on the quality of separation.

arrival (DOA) for three different noise levels  $\sigma_N^2 = -15$  dB,  $-5$  dB, and  $5$  dB. The dotted line is the theoretical upper bound of performance of [2, eq. 30].

Fig. 4 is the analogous plot for the RMSE of the reconstruction of the mixing matrix.

Thus far, the results obtained by STOTD turn out to be nearly the same as the results of the JADE algorithm. The computational load of JADE and STOTD are comparable as well. In the real case, the computation of the optimal vector  $U$  leads to the rooting of a quadratic polynomial in both methods. In the complex case, both methods lead to the rooting of a polynomial of degree 3. The only difference consists of the fact that in the JADE algorithm, one usually restricts the number of matrix slices that are processed to  $J$  by computing the  $J$ -dimensional dominant subspace of a Hermitian (symmetric) ( $J^2 \times J^2$ ) matrix; the other eigenvectors are considered to be noise contributions. In the STOTD tech-

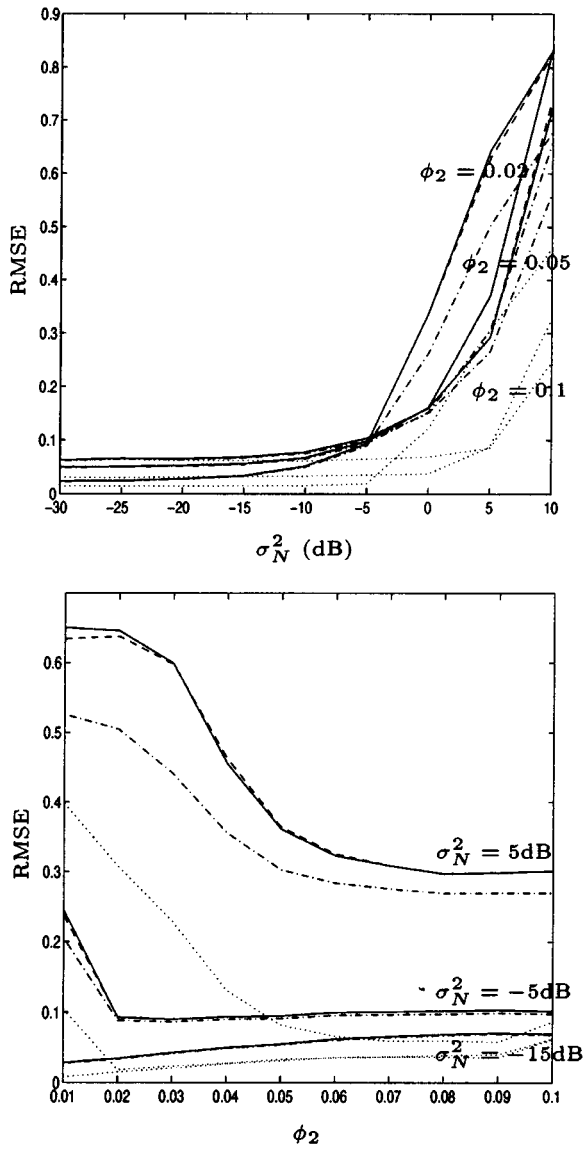


Fig. 4. RMSE between the true mixing matrix and its estimate in the second simulation of Section III-D. Solid: The mixing matrix is estimated by means of the STOTD technique. Dashed: The mixing matrix is estimated by means of the JADE technique. Dash-dotted: The upper-bound of performance given by [10, eq. (20)]. Dotted: The upper-bound of performance given by [10, eq. (21)]. *Top*: Effect of the SNR on the quality of the reconstruction.  $\phi_1 = 0$ . *Bottom*: Effect of the difference in DOA ( $\phi_1 = 0$ ) on the quality of the reconstruction.

nique, such a reduction step is not required (although the “fuzzy” reduction of (42) may still make sense).

The third experiment is similar to the second, except that there are three sources instead of two. The electrical angle of the third source is assumed to be  $\phi_3 = \phi_2/2$ . The iteration stops when for all the Jacobi rotation matrices computed in the same sweep, the off-diagonal entries are smaller than  $1e-3$  in absolute value. The obtained accuracy is measured in terms of the index [12]

$$\frac{1}{2} \left[ \sum_i \left( \sum_j \frac{|s_{ij}|^2}{\max_l |s_{il}|^2} - 1 \right) \times \sum_j \left( \sum_i \frac{|s_{ij}|^2}{\max_l |s_{lj}|^2} - 1 \right) \right] \quad (60)$$

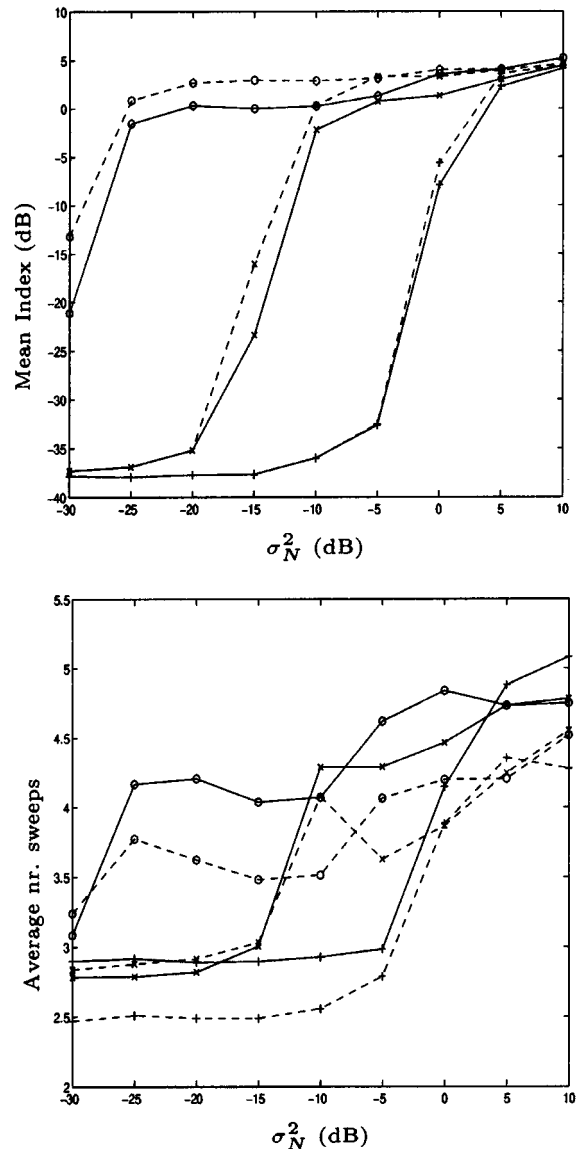


Fig. 5. Mean index (top) and number of sweeps (bottom) as a function of the SNR in the third simulation of Section III-D. Solid: The mixing matrix is estimated by means of the STOTD technique. Dashed: The mixing matrix is estimated by means of the JADE technique.  $\phi_1 = 0$ . “o”-marks:  $\phi_2 = 0.02$ . “x”-marks:  $\phi_2 = 0.05$ . “+”-marks:  $\phi_2 = 0.1$ .

in which  $\mathbf{S} = \hat{\mathbf{M}}^\dagger \mathbf{M}$ . This index is zero if  $\hat{\mathbf{M}}$  equals  $\mathbf{M}$  up to a column scaling and permutation, and a small value indicates that the estimate is close.

In Figs. 5 and 6, we plot the index value and the required number of sweeps averaged over 500 Monte Carlo runs. We note that the accuracy obtained with the STOTD technique is generally a bit higher than with the JADE technique, especially for problems that are a bit more challenging; however, the JADE iterations stopped after a somewhat smaller number of sweeps. On the average, the convergence is fast. We remark that generally more sweeps may be needed when the problem becomes more difficult. We checked whether the higher accuracy of STOTD was due to the stop criterion, i.e., whether JADE would not yield the same accuracy if more iterations were allowed. This turned out not to be the case. When in each

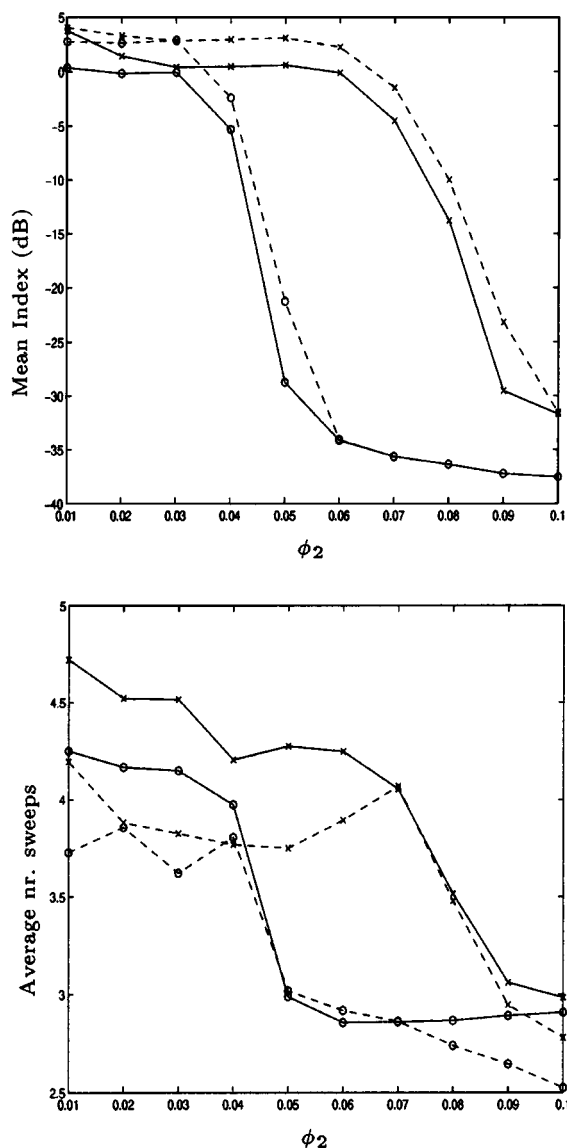


Fig. 6. Mean index (top) and number of sweeps (bottom) as a function of  $\phi_2$  in the third simulation of Section III-D.  $\phi_1 = 0$ . Solid: The mixing matrix is estimated by means of the STODD technique. Dashed: The mixing matrix is estimated by means of the JADE technique. “o”-marks:  $\sigma_N^2 = -15$  dB. “x”-marks:  $\sigma_N^2 = -5$  dB.

run five extra JADE sweeps were carried out, the maximal improvement of index (60), which was considered over all runs, was smaller than 3%.

If we analyze the simulation results in detail, then we see that there are runs in which STODD was able to find a good solution, whereas JADE was not, and vice versa. For instance, the maximum number of iterations required by STODD (47) was for a run where  $\phi_2 = 0.1$  and  $\sigma_N^2 = 0$  dB; the obtained index value was 0.45, whereas JADE obtained a value of 0.003 in seven sweeps. On the other hand, under the same conditions, there was a run where JADE needed 32 iterations to obtain an index value of 0.42, whereas STODD converged to a value of 0.002 in three sweeps.

Apparently, in these two cases, one of the two methods did not converge to the global optimum. As an indication of how often

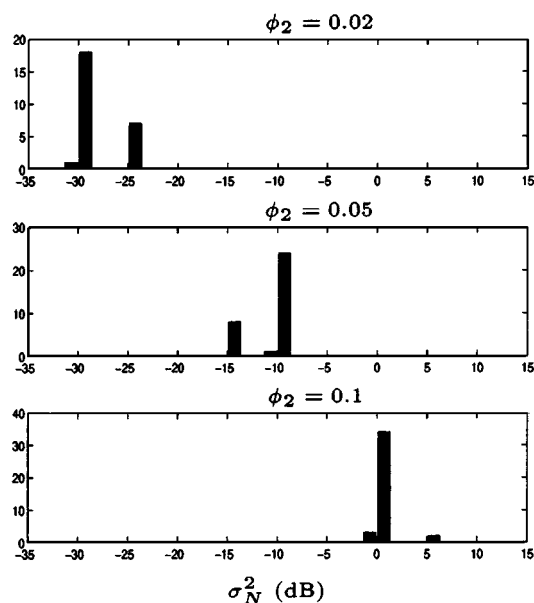


Fig. 7. Number of runs in the third simulation of Section III-D, where the index obtained with STODD was more than 50 times the index obtained with JADE (bars left from the value of  $\sigma_N^2$ ) or vice versa (bars right from the value of  $\sigma_N^2$ ).

this happens, we plot in Fig. 7 the number of runs in which the index (60) obtained with the STODD technique was more than 50 times the index obtained with the JADE technique, and vice versa. In these runs, either STODD or JADE was not globally converging or at least the convergence speed became too slow. In our experiment, this was significantly more often the case for JADE than for STODD.

We also mention that in [14] an experiment was conducted in which STODD and JADE were based on third- and fourth-order cumulants and where it was concluded that the STODD results were better for sources with a positive kurtosis, whereas the JADE results were better for sources with a negative kurtosis.

#### IV. CONCLUSION

We have proved that the computation of an elementary Jacobi rotation, in the optimal diagonalization of a third-order cumulant, can be formulated as the best rank-1 approximation of a real symmetric ( $2 \times 2$ )-matrix (real case) or ( $3 \times 3$ )-matrix (complex case). This is still true for the optimal diagonalization of a set of third-order cumulants; the matrix is obtained as a sum of contributions of the individual tensors in the set. Comparison with formulas for simultaneous matrix diagonalization leads to the result that simultaneous diagonalization of complex (real) third-order tensors exhibiting the symmetry specified in Section II is similar to the simultaneous diagonalization of Hermitian (symmetric) matrices.

We have shown that ICA can be realized by simultaneous diagonalization of third-order tensors, spanning the range of the standardized fourth-order cumulant. This algorithm is similar in spirit to the JADE algorithm. We have interpreted the algorithm in terms of contrast optimization and proved that it corresponds to an invariant ICA estimator.



APPENDIX A  
PROOFS

*Theorem 1:*

*Proof:* The diagonal entries of  $\mathcal{C}$  have the form

$$\begin{aligned} c_{111} &= \cos^3 \alpha \tilde{c}_{111} - 3 \cos^2 \alpha \sin \alpha \tilde{c}_{112} \\ &= +3 \cos \alpha \sin^2 \alpha \tilde{c}_{122} - \sin^3 \alpha \tilde{c}_{222}, \\ c_{222} &= \sin^3 \alpha \tilde{c}_{111} + 3 \sin^2 \alpha \cos \alpha \tilde{c}_{112} \\ &= +3 \sin \alpha \cos^2 \alpha \tilde{c}_{122} + \cos^3 \alpha \tilde{c}_{222}. \end{aligned}$$

The squared diagonal norm of  $\mathcal{C}$  can then be written as

$$\begin{aligned} c_{111}^2 + c_{222}^2 &= \left( \frac{9}{4} (\tilde{c}_{112}^2 + \tilde{c}_{122}^2) \right. \\ &\quad \left. + \frac{3}{2} (\tilde{c}_{111} \tilde{c}_{122} + \tilde{c}_{112} \tilde{c}_{222}) \right) \sin^2(2\alpha) \\ &\quad + (\tilde{c}_{111}^2 + \tilde{c}_{222}^2) \left( 1 - \frac{3}{4} \sin^2(2\alpha) \right) \\ &\quad + (\tilde{c}_{122} \tilde{c}_{222} - \tilde{c}_{111} \tilde{c}_{112}) (3 \sin(2\alpha) \cos(2\alpha)). \end{aligned}$$

In (14), this expression is given in a matrix format. ■

*Theorem 2:*

*Proof:* The diagonal entries of  $\mathcal{C}$  have the form

$$\begin{aligned} c_{111} &= \cos^3 \alpha \tilde{c}_{111} - \cos^2 \alpha \sin \alpha (2\tilde{c}_{112} e^{-i\phi} + \tilde{c}_{211} e^{i\phi}) \\ &\quad + \cos \alpha \sin^2 \alpha (\tilde{c}_{122} e^{-2i\phi} + 2\tilde{c}_{212}) - \sin^3 \alpha \tilde{c}_{222} e^{-i\phi} \\ c_{222} &= \sin^3 \alpha \tilde{c}_{111} e^{i\phi} + \sin^2 \alpha \cos \alpha (2\tilde{c}_{112} + \tilde{c}_{211} e^{2i\phi}) \\ &\quad + \sin \alpha \cos^2 \alpha (\tilde{c}_{122} e^{-i\phi} + 2\tilde{c}_{212} e^{i\phi}) + \cos^3 \alpha \tilde{c}_{222}. \end{aligned}$$

The squared diagonal norm of  $\mathcal{C}$  can then be written as

$$\begin{aligned} |c_{111}|^2 + |c_{222}|^2 &= |\tilde{c}_{111}|^2 + |\tilde{c}_{222}|^2 \\ &\quad + \sin^2(2\alpha) \left[ -\frac{3}{4} (|\tilde{c}_{111}|^2 + |\tilde{c}_{222}|^2) \right. \\ &\quad \left. + \frac{1}{4} (|2\tilde{c}_{112} + \tilde{c}_{211} e^{2i\phi}|^2 + |2\tilde{c}_{212} + \tilde{c}_{122} e^{-2i\phi}|^2) \right. \\ &\quad \left. + \frac{1}{2} \operatorname{Re}(\tilde{c}_{111} (\tilde{c}_{122} e^{-2i\phi} + 2\tilde{c}_{212})^* \right. \\ &\quad \left. + \tilde{c}_{222} (\tilde{c}_{211} e^{2i\phi} + 2\tilde{c}_{112})^*) \right] \\ &\quad - \sin(2\alpha) \cos(2\alpha) \operatorname{Re}(\tilde{c}_{111} e^{i\phi} (\tilde{c}_{211} e^{2i\phi} + 2\tilde{c}_{112})^* \\ &\quad - \tilde{c}_{222}^* e^{i\phi} (\tilde{c}_{122} e^{-2i\phi} + 2\tilde{c}_{212})). \end{aligned}$$

In (36), this expression is reorganized and presented in a matrix format. ■

*Theorem 3:*

*Proof:* Define  $\tilde{X} = \mathbf{Q}X$ , in which  $X$  has mutually independent components, and  $\mathbf{Q}$  is unitary (orthogonal). We will prove that  $f(\tilde{X}) \leq f(X)$  and that the equality sign only holds if  $\mathbf{Q} = \mathbf{A}\mathbf{P}$ , in which  $\mathbf{A}$  is a diagonal matrix of unit-norm elements, and  $\mathbf{P}$  is a permutation.

Since the components of  $X$  are mutually independent, its fourth-order cumulant is diagonal, and  $f(X)$  is the squared Frobenius-norm of this cumulant (the squared Frobenius-norm of a tensor is by definition the sum of the squares of all its entries)

$$f(X) = \sum_{j=1}^J \left| (c_4^X)_{jjjj} \right|^2 = \|c_4^X\|^2.$$

On the other hand, we remind that the cumulant of  $\tilde{X}$  is given by

$$c_4^{\tilde{X}} = c_4^X \times_1 \mathbf{Q} \times_2 \mathbf{Q}^* \times_3 \mathbf{Q}^* \times_4 \mathbf{Q}.$$

$f(\tilde{X})$  can be bounded by the squared Frobenius-norm of  $c_4^{\tilde{X}}$  to prove that  $f(\tilde{X}) \leq f(X)$ :

$$\begin{aligned} f(\tilde{X}) &= \sum_{j,l} \left| (c_4^{\tilde{X}})_{jjjl} \right|^2 \leq \|c_4^{\tilde{X}}\|^2 \\ &= \|c_4^X\|^2 = f(X) \end{aligned}$$

in which we used that the fact that multiplication with a unitary matrix does not alter the Frobenius norm of a tensor.

Now, we prove that the equality sign only holds if  $\mathbf{Q}$  is of the form specified above. Let us first assume that all the components of  $X$  are kurtic.  $f(\tilde{X}) = f(X)$ , or  $f(\tilde{X}) = \|c_4^{\tilde{X}}\|^2$  implies that the third-order cumulant slices of  $c_4^{\tilde{X}}$ , which are represented by  $(c_4^{\tilde{X}})^{(l)}$ , are strictly diagonal, e.g., the first tensor slice is given by

$$(c_4^{\tilde{X}})^{(1)}_{i_1 i_2 i_3} = \sum_j (q_{1j} \kappa^{x_j}) q_{i_1 j} q_{i_2 j}^* q_{i_3 j}^*.$$

Now, assume that exactly  $F > 1$  of these terms do not vanish (say  $q_{11} \kappa^{x_1} \neq 0, q_{12} \kappa^{x_2} \neq 0, \dots, q_{1F} \kappa^{x_F} \neq 0$ ). According to a property of higher order tensors (cf. [9, th. 7.3.3]), claiming that  $(c_4^{\tilde{X}})^{(1)}$  is strictly diagonal means that the matrix  $\mathbf{Q}_{1:F} = [Q_1 Q_2 \dots Q_F]$  with  $Q_j$  representing the  $j$ th column of  $\mathbf{Q}$ , is in the form

$$\mathbf{Q}_{1:F} = \tilde{\mathbf{A}} \tilde{\mathbf{P}}$$

in which  $\tilde{\mathbf{A}} \in \mathbb{C}^{J \times F}$  contains  $F$  unit-norm elements on the diagonal, and  $\tilde{\mathbf{P}} \in \mathbb{C}^{F \times F}$  is a permutation. However, this implies that only one of the coefficients  $q_{1f} \kappa^{x_f}$  ( $1 \leq f \leq F$ ) could have been different from zero. Hence, we conclude that diagonality of  $(c_4^{\tilde{X}})^{(1)}$  involves that  $F = 1$ . In other words, the first row of  $\mathbf{Q}$  only contains one nonzero entry; this entry has unit norm. Repeating the derivation for the other third-order cumulant slices, and taking into account that  $\mathbf{Q}$  is unitary, shows that  $\mathbf{Q}$  contains exactly one unit-modulus entry in each column and each row.

Finally, if, e.g.,  $x_j$  is nonkurtic, then the reasoning above can be repeated for the random vector formed by the first  $J-1$  components of  $X$ . The fact that the original  $\mathbf{Q}$  has to be orthogonal then induces the required form of the remaining column  $Q_J$ . ■

*Theorem 4:*

*Proof:* Call  $\hat{X}$  the estimate of the source vector  $X$  with estimated covariance  $\hat{\mathbf{C}}^{\hat{X}}$  and cumulant  $\hat{c}_4^{\hat{X}}$ . The prewhitening takes the form of  $\hat{\mathbf{C}}^{\hat{X}} = \mathbf{I}$ , and the higher order step is based on the optimization of  $\sum_{l,j} |(c_4^{\hat{X}})_{jjjl}|^2$ . Hence, the algorithm is based on the output of the separator, which is a sufficient condition for invariance [3]. ■

REFERENCES

- [1] J.-F. Cardoso and A. Souloumiac, "Blind beamforming for nongaussian signals," in *Proc. Inst. Elect. Eng. F*, vol. 140, 1994, pp. 362–370.
- [2] J.-F. Cardoso, "On the performance of orthogonal source separation algorithms," in *Proc. EUSIPCO*, vol. 2, Edinburgh, U.K., Sept. 13–16, 1994, pp. 776–779.

- [3] —, “The invariant approach to source separation,” in *Proc. NOLTA*, Las Vegas, NV, Dec. 10–14, 1995, pp. 55–60.
- [4] —, “High-order contrasts for independent component analysis,” *Neural Comput.*, vol. 11, no. 1, pp. 157–192, 1999.
- [5] P. Comon, “Tensor diagonalization, a useful tool in signal processing,” in *Proc. 10th IFAC Symp. Syst. Iden.*, vol. 1, Copenhagen, Denmark, July 4–6, 1994, pp. 77–82.
- [6] —, “Independent component analysis. A new concept?,” *Signal Process.*, vol. 36, no. 3, pp. 287–314, Apr. 1994. Special Issue *Higher Order Statistics*.
- [7] L. De Lathauwer, P. Comon, B. De Moor, and J. Vandewalle, “Higher-order power method—Application in independent component analysis,” in *Proc. Int. Symp. Nonlinear Theory Applicat.*, vol. 1, Las Vegas, NV, Dec. 10–14, 1995, pp. 91–96.
- [8] L. De Lathauwer, B. De Moor, and J. Vandewalle, “Blind source separation by simultaneous third-order tensor diagonalization,” in *Proc. EUSIPCO*, vol. 3, Trieste, Italy, Sept. 10–13, 1996, pp. 2089–2092.
- [9] L. De Lathauwer, “Signal Processing Based on Multilinear Algebra,” Ph.D. thesis, Elect. Eng. Dept., Katholieke Univ. Leuven, Leuven, Belgium, 1997.
- [10] L. De Lathauwer, B. De Moor, and J. Vandewalle, “A residual bound for the mixing matrix in ICA,” in *Proc. EUSIPCO*, Rhodes, Greece, Sept. 8–11, 1998, pp. 2065–2068.
- [11] E. L. Lehmann, *Testing Statistical Hypotheses*. New York: Wiley, 1959.
- [12] E. Moreau, “Criteria for complex sources separation,” in *Proc. EUSIPCO*, Trieste, Italy, Sept. 10–13, 1996, pp. 931–934.
- [13] E. Moreau and N. Thirion-Moreau, “Nonsymmetrical contrasts for sources separation,” *IEEE Trans. Signal Processing*, vol. 47, pp. 2241–2252, Aug. 1999.
- [14] E. Moreau, “A generalization of joint-diagonalization criteria for source separation,” *IEEE Trans. Signal Processing*, submitted for publication.
- [15] B. Stoll and E. Moreau, “A generalized ICA algorithm,” *IEEE Signal Processing Lett.*, vol. 7, pp. 90–92, Apr. 2000.



**Lieven De Lathauwer** was born in Aalst, Belgium, on November 10, 1969. He received the degree in electro-mechanical engineering in 1992 and the doctoral degree in applied sciences in 1997, both from the Katholieke Universiteit Leuven (KU Leuven), Leuven, Belgium. His Ph.D. thesis concerned signal processing based on multilinear algebra.

He is currently with the French Centre National de la Recherche Scientifique (CNRS), Cergy-Pontoise, France; he also holds a honorary post-doctoral research mandate with the Fund for Scientific Research-Flanders (FWO), which is affiliated with the KU Leuven. His research interests include linear and multilinear algebra, statistical signal and array processing, higher order statistics, ICA and BSS, identification, blind identification, and equalization.



**Bart De Moor** (SM'93) was born in Halle, Brabant, Belgium, on July 12, 1960. He received the doctoral degree in applied sciences in 1988 from the Katholieke Universiteit Leuven (KU Leuven), Leuven, Belgium.

He was a Visiting Research Associate with the Department of Computer Science and Electrical Engineering, Stanford University, Stanford, CA, from 1988 to 1989. Since 1989, he has been with the Electrical Engineering Department, KU Leuven, where he has been a Full Professor since 2000. His research interests include numerical linear algebra, system identification, control theory, and signal processing. He has more than 200 papers in international journals and conference proceedings. From 1991 to 1992, he was the Chief of Staff of the Belgian Federal Minister of Science W. Demeester-DeMeyer and, later, of the Belgian Prime Minister W. Martens. From 1994 to 1999, he was the main advisor on science and technology policy to the Flemish Minister-President L. Van den Brande.

Dr. De Moor received the Leybold-Heraeus Prize in 1986, the Leslie Fox Prize in 1989, the Guillemin-Cauer Best Paper Award of the IEEE TRANSACTIONS ON CIRCUITS AND SYSTEMS in 1990, the bi-annual Siemens prize in 1994, and he became a Laureate of the Belgian Royal Academy of Sciences in 1992. He is a member of several boards of administrators of (inter)national scientific, cultural, and commercial organizations, including the Belgian Institute for Control and Automation, the Flemish Interuniversity Institute for Biotechnology, and the spin-off companies ISMC NV and Data4s NV.



**Joos Vandewalle** (F'92) received the doctoral degree in applied sciences in 1976 and the special doctoral degree in 1984 from the Katholieke Universiteit Leuven (KU Leuven), Leuven, Belgium.

He was a postdoctoral researcher from 1976 to 1978 and a Visiting Assistant Professor from 1978 to 1979 with the Electrical Engineering and Computer Science Department, University of California, Berkeley. Since 1979, he has been with the Electrical Engineering Department, KU Leuven, where he has been a Full Professor since 1986. His main research interests are in system theory and its applications in circuit theory, signal processing, cryptography, and neural networks. He is currently Vice-Dean of the Faculty of Applied Sciences, KU Leuven. He is also head of the Research Group SISTA-COSIC-DocArch of the Department of Electrical Engineering ESAT at the KU Leuven. He is one of the three coordinators of the Interdisciplinary Center for Neural Networks (ICNN), which is regrouping some 50 researchers at the KU Leuven. In 1992, he held the Franquai chair on neural networks at the Université de Liège, Liège, Belgium.

Dr. Vandewalle is currently Vice President for Region 8 of the IEEE Society on Circuits and Systems.